XVIII IMEKO WORLD CONGRESS
Metrology for a Sustainable Development
September, 17 – 22, 2006, Rio de Janeiro, Brazil

ANISOTROPY OF STEEL SHEETS AND CONSEQUENCE FOR EPSTEIN TEST: I THEORY

Marcos Flavio de Campos

INMETRO - DIMCI/DIMAT, Av. Nossa Senhora das Graças 50 Xerém - Duque de Caxias RJ, BRASIL, mfcampos@inmetro.gov.br

Abstract: ODF – Orientation Distribution Function – Theory allow the prediction of the average magnetic properties of electrical steels when crystalline symmetry of cubic bcc iron and the orthorhombic sheet symmetry are taken into account. The crystallographic texture can be related to the magnetocrystalline anisotropy by means of a very simple expression. The dependence of the variables: Magnetic Induction, coercivity, permeability and iron losses with texture is discussed. Magnetic Induction at high fields - B_{25} and B_{50} - can be directly scaled to magnetocrystalline anisotropy. Effects of demagnetizing field on the Magnetic Induction are commented. Permeability and power losses are not directly related to magnetocrystalline anisotropy, mainly due the existence of domain wall displacement phenomena. The domain wall structure is function of the crystalline orientation and also contributes for the anisotropy of iron losses. As consequence of the theoretical analysis, it is suggested that the traditional Epstein arrangement (50% RD-Rolling Direction plus 50% TD–Transverse Direction), be changed for 3 separate measurements in the RD, TD (i.e., 90^o) and 45^o directions.

Keywords: electrical steels, anisotropy, magnetic induction, permeability, energy losses.

1. INTRODUCTION

Non-oriented electrical steels are silicon alloyed steels employed in rotating machines, and ideally should not present anisotropy.

However, the commercial non-oriented electrical steels typically present significant anisotropy of magnetic properties [1,2]. This is due to the microstructure, and the main reason is that the Goss texture component (110) [001] is one of the most important texture components in recrystallized bcc iron [3,4]. The presence of Goss implies in better magnetic properties at rolling direction of the sheets, and worse magnetic properties at 54.7^o of the rolling direction [5].

Standards like the North-American ASTM A 343 [6] or Brazilian NBR 5161 [7] specify for the Epstein test that 50% of the sheets are from rolling direction (RD, or 0^o) and 50% are from transverse direction (TD, or 90^o).

As consequence of presence of Goss component, the arrangement used in Epstein test (50%RD+50%TD) typically overestimates the average result for steels. Penin et al [1] recently suggested performing measurements at 45^o of RD as a method to reduce the discrepancy.

The objective of this paper is to show there is theoretical basis for the suggestions by Penin et al [1]. This is obtained by means of the ODF (Orientation Distribution Function) [8].

As consequence of crystalline symmetry (bcc iron cubic symmetry) and orthorhombic sheet symmetry, an expression of the type $A_o = (A(0^o)+A(90^o)+2A(45^o))/4$ – where A is an arbitrary variable - can describe, at least as first approximation, the average physical properties of a steel sheet. Better results are obtained for 4^{th} order properties, which can be described by the three first ODF coefficients [8,9]. This is, for example, the case of B_{50} (Magnetic Induction for a field H= 5000 A/m), which - in a non-plastically deformed steel – can be considered direct function of K_1, the magnetocrystalline anisotropy constant. The possibility of using this model for describing anisotropy of power losses and permeability is also discussed.

2. THEORY FOR ANISOTROPY

A physical property (for example, mechanical or magnetic) can be described by the three first ODF coefficients since it is a 4^{th} order property [8,9], according equation (1):

$$A = A_o + A_1 \cos(2\beta) + A_2 \cos(4\beta) \qquad (1)$$

where the average - A_o – can be experimentally found by equation (2). The other constants of equation (1), A_1 and A_2 are experimentally, respectively, with equations (3) and (4)

$$A_0 = \frac{1}{4}\left[A(0^0) + A(90^0) + 2 \cdot A(45^0)\right] \qquad (2)$$

$$A_1 = \frac{1}{2}\left[A(0^0) - A(90^0)\right] \qquad (3)$$

$$A_2 = \frac{1}{4}\left[A(0^0) + A(90^0) - 2 \cdot A(45^0)\right] \qquad (4)$$

2.1. Magnetic Anisotropy

The magnetocrystalline anisotropy energy E_A can be written as function of the anisotropy constants K_1, K_2, as shown in equation (5):

$$E_A = K_0 + K_1(\omega_1^2\omega_2^2 + \omega_1^2\omega_3^2 + \omega_2^2\omega_3^2) + K_2(\omega_1^2\omega_2^2\omega_3^2) \quad (5)$$

The equations (functions (6) and (7)) present cubic symmetry.

$$\xi_1(\omega) = \omega_1^2\omega_2^2 + \omega_1^2\omega_3^2 + \omega_2^2\omega_3^2 \quad (6)$$

$$\xi_2(\omega) = \omega_1^2\omega_2^2\omega_3^2 \quad (7)$$

The equations (6) and (7) are related to spherical harmonics in the following way [8]:

$$\xi_1(\omega) = \frac{1}{5}\frac{\dot{k}_4^1(\omega)}{n_4} + \frac{1}{5} \quad (8)$$

$$\xi_2(\omega) = \frac{1}{231}\frac{\dot{k}_6^1(\omega)}{n_6} + \frac{1}{55}\frac{\dot{k}_4^1(\omega)}{n_4} + \frac{1}{105} \quad (9)$$

with $n_4 = 0.64636$ and $n_6 = 0.359601$ (see Bunge [8])

Equation (5) can be rewritten (not taking into account the term related to K_0):

$$E(\omega) = \frac{\dot{k}_4^1(\omega)}{n_4}\left[\frac{K_1}{5} + \frac{K_2}{55}\right] + \frac{\dot{k}_6^1(\omega)}{n_6}\frac{K_2}{231} \quad (10)$$

It is assumed sample with orthorhombic symmetry (sheet symmetry), the expression (13). The surface spherical harmonics are given, for this symmetry:

$$\dot{k}_l^1 = \frac{1}{\sqrt{2\pi}}\overline{P}_l(\Phi) \quad (11)$$

$$\dot{k}_l^\nu = \frac{1}{\sqrt{\pi}}\overline{P}_l^{2(\nu-1)}(\Phi)\cdot\cos(2(\nu-1)\cdot\beta) \quad (12)$$

then expression (10) becomes:

$$\overline{E}(\Phi,\beta) = \frac{1}{9n_4\sqrt{\pi}}\left[\frac{K_1}{5} + \frac{K_2}{55}\right]\cdot F_4(\Phi,\beta) + \frac{1}{13n_6\sqrt{\pi}}\frac{K_2}{231}\cdot F_6(\Phi,\beta) \quad (13)$$

with the 4th order texture expressed as (equation (14)):

$$F_4(\Phi,\beta) = \frac{1}{\sqrt{2}}C_4^{11}\overline{P}_4^0(\Phi) + C_4^{12}\overline{P}_4^2(\Phi)\cos 2\beta + C_4^{13}\overline{P}_4^4(\Phi)\cos 4\beta \quad (14)$$

and 6th order texture parameter given by:

$$F_6(\Phi,\beta) = \frac{1}{\sqrt{2}}C_6^{11}\overline{P}_6^0(\Phi) + C_6^{12}\overline{P}_6^2(\Phi)\cos 2\beta + C_6^{13}\overline{P}_6^4(\Phi)\cos 4\beta + C_6^{14}\overline{P}_6^6(\Phi)\cos 6\beta \quad (15)$$

For the sheet plane, $\Phi=90^o$. $\overline{P}_l^q(\Phi)$ (q=0,2,4,6 and l =4,6) are the normalized associated Legendre functions [8].

The contribution of K_2 in the equation (13) can be considered negligible. K_2 is one order of magnitude lower than K_1 [10].

If the possible contribution of K_2 can be neglected, then the magnetic induction B is directly proportional to $F_4(90^o,\beta)$, and this procedure was adopted by several authors [11,12]. Thus, E_A can be written as function of only cos 2β and cos 4β, (see equation 1).

Then, (emphasizing that this is only valid for rotation of the magnetization of domains) the induction B (that is direct function of the anisotropy energy E_A), can be written by the equation (16), which is a modification of equation (14) with $\Phi=90^o$:

$$B(\beta) = a + b[-1.091\cdot C_4^{11} + 1.6266\cdot C_4^{12}\cdot\cos(2\beta) - 2.1516\cdot C_4^{13}\cdot\cos(4\beta)] \quad (16)$$

According this simple model, the experimental measurement for only two directions is sufficient for finding the constants *a* and *b* of equation (16).

It is relevant to add that the deduction that leads to equations (14) and (16) show the validity of equation (1), which applies for 4th order properties [8]. Equation (1) indicates that with the measurement for 0°, 45° and 90° we obtain the average properties, and this can be used as approximation even for higher order (above 4th) properties.

2.2. Graphic Representation

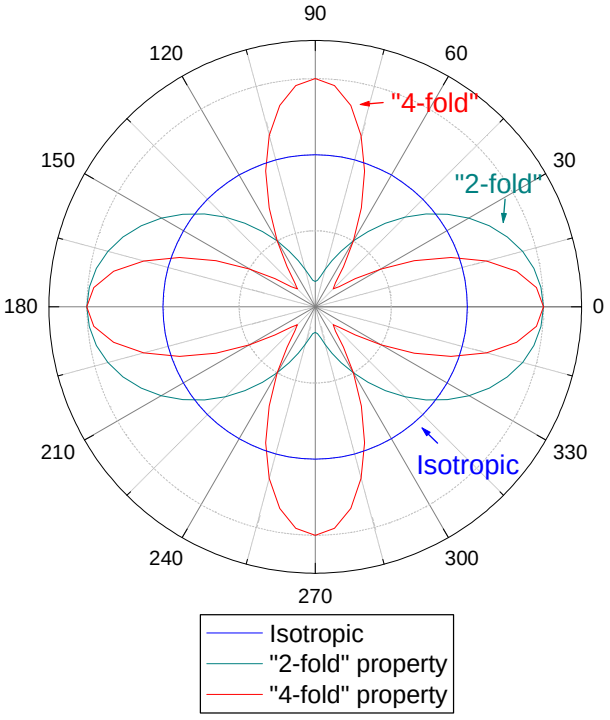

Fig. 1. Graphic representation of the terms of the equation $A = A_o + A_1 \cos(2\beta) + A_2 \cos(4\beta)$, see also Table 1.

Equation (1) can be graphically represented, as suggested by Bunge [9,13], see figure 1. In the Table 1 we can see the correspondence between Eq. (1) and Eq. (16).

Fig. 1 is useful to understand the relationship between ODF coefficients and physical properties. Bunge [9,13] calls "2-fold" a property that varies according cos 2β, and "4 fold" a property that varies according cos 4β, see Fig.1 and Table 1.

Table 1. Relation between ODF coefficients and terms of expression $A = A_o + A_1 \cos(2\beta) + A_2 \cos(4\beta)$

A (β) =	A_0	+ A_1 cos (2β)	+ A_2 cos (4β)
	constant	"2-fold"	"4-fold"
	$\sim C_4^{11}$	$\sim C_4^{12}$	$\sim C_4^{13}$

3. EVALUATION OF PHYSICAL PROPERTIES

The previous section discussed how a simplified model (equation 1) can be used to estimate and represent anisotropy (magnetocrystalline anisotropy, in particular). The purpose of the following sections is discussing if this simple model is valid for describing several different properties like Magnetic Induction, permeability and iron losses.

In other words, can these properties (Magnetic Induction, permeability and iron losses) be scaled to magnetocrystalline anisotropy energy?

3.1. Angular dependence of Magnetic Induction

It has been experimentally shown [14,15] that Magnetic Inductions B_{50} (for H=5000 A/m) or B_{25} (for H=2500 A/m) can be scaled to the Anisotropy Energy (Eq. 5). However, other details were not taken into account [14,15], among them mainly those due to demagnetizing fields. A more rigorous deduction of the dependence of Magnetic Induction with crystalline orientation will be presented in this section. This is the Theory of Magnetization of single crystals, also known as Neél phase Theory [16], which also is not totally complete, because only takes into account domain rotation, neglecting the existence of domain walls. The Neél phase theory is as follows:

The energy corresponding to the applied field H is (Eq. 17):

$$E_H = - Js\, H \cos\psi \quad (or\ E_H = - \mu_o\, Ms\, H \cos\psi) \qquad (17)$$

where E is energy, H is applied field, Js the polarization of saturation, Ms the magnetization of de saturation, $J=\mu_o M$. ψ is the angle between magnetization and applied magnetic field.

The torque due to the magnetic field H acting on the sample (Eq. 17) is opposed by the torque due to the magnetocrystalline anisotropy (Equation 5), resulting in Eq. (18).

$$J_s H \sin\psi = \frac{dE_A}{d\psi} \qquad (18)$$

with $M=\cos\psi\, Ms$ and $m = M/Ms = J/Js = \cos\psi$.

The solution of Equation (18) is not simple. The main difficulty is the existence of three different vectors: Magnetization, Applied Field, and the easy axis of the crystal. The direction of the magnetization vector will depend on the *shape* of the crystal. In other words, the direction –and value – of the Magnetization will be function of the demagnetizing field, which only can be known exactly if the shape of the crystal is ellipsoid.

The <100>, <110> e <111> directions are particular cases, where (due to symmetry) the resultant magnetization vector has the same direction of the applied field [17,18]. For these cases, the magnetization in *H* direction is $\mu_o\, Ms \cos\psi$, resulting $m = M/Ms = J/Js$.

i) <100> direction
for infinitesimal H saturation is already attained.

ii) <110> direction

$$H = (4K_1 / Js)\, m\, [m^2 - (1/2)] \qquad (19)$$

iii) <111> direction

$$H = (K_1 / 3Js)\, [(2 - 2m^2)^{1/2}\, (4m^2 - 1) + m\, (7m^2 - 3)] + (K_2 / 18Js)\, [m\, (23m^4 - 16m^2 + 1) - (2 - 2m^2)^{1/2}\, (10m^4 - 9m^2 + 1)] \qquad (20)$$

The equations that describe the magnetization curve for 3 vectors and 2 vectors regions are [19,20]:

3 vectors Region:

$$M = \sqrt{3}\ M_{[111]}(H) / (\upsilon_1 + \upsilon_2 + \upsilon_3) \qquad (21)$$

$$Ha = (\upsilon_1 + \upsilon_2 + \upsilon_3)\, H / \sqrt{3} \qquad (22)$$

where υ_1, υ_2, υ_3 are direction cosines of the applied field. The magnetization curve remains in the 3 vectors region until two of the magnetization vectors become coplanar with Ha.

2 vectors Region:

Defining the τ and ϕ angles as:

$$\sqrt{2}\ \omega_1 = \cos\tau \cos\phi \pm \sin\phi \qquad (23a)$$

$$\sqrt{2}\ \omega_2 = \cos\tau \cos\phi \mp \sin\phi \qquad (23b)$$

$$\omega_3 = \sin\tau \cos\phi \qquad (23c)$$

where ω_1, ω_2 and ω_3 are cosines of magnetization vector to easy axis, see Eq. (5), we get:

$$\sin\tau = \upsilon_3 [2/(2-(\upsilon_1-\upsilon_2)^2)]^{1/2} \qquad (24)$$

$$\cos\zeta = (\upsilon_1+\upsilon_2)(\cos\tau/\sqrt{2}) + \upsilon_3 \sin\tau \qquad (25)$$

$$M_{[2\ vectors]} = Ms\, (\cos\phi / \cos\zeta) \qquad (26)$$

Now, using equation (5), with the angles ω_1 ω_2 ω_3 defined above, and making: $(\partial E / \partial\phi)_\theta = 0$, it is obtained:

$$Ha\, Js\, (\sin\phi / \cos\zeta) = - (K_1/2) \sin 2\phi\, [\sin^2\phi\, (1+\cos^2\tau) - 2\sin^2\tau + \cos^2\phi\, (4\sin^4\phi - \cos^2\phi - \cos^4\phi)] + (K_2/4) \sin^2\tau \sin 2\phi\, [\cos^2\phi\, (1+\cos^2\tau) - 1]\, [3\cos^2\phi\, (1+\cos^2\tau) - 1] \qquad (27)$$

Equation (27) gives the value of variable ϕ. Eq. (27) is solved trying different values of ϕ, until the solution is found (trial and error). The value found for ϕ is placed in the equation (26) to get the magnetization in the 2 vectors region.

Table .2. Planes of bcc iron considered for calculation

Plane	Convention of directions	
	0°	90°
(100)	[100]	[010]
(310)	[100]	$[0\bar{3}1]$
(110)	[100]	[011]
(211)	$[\bar{1}11]$	$[01\bar{1}]$
(111)	$[\bar{2}11]$	$[0\bar{1}1]$

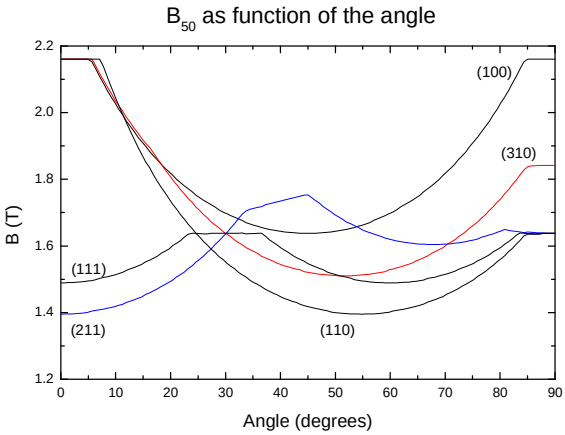

Fig. 2. Magnetic Induction B_{50} for several planes, see Table 2 for convention code. Calculations done for pure iron, B=2.16 T, K_1 = 4.8 10^4 J/m^3.

Fig. 2 shows the result of application of the model, Eq. (18) to (27) for several crystalline planes of iron.

The general formula for the demagnetizing field is Nx+Ny+Nz=1. In the case of a sheet, or flat plate, the dimension of thickness is very small compared with the others. Thus we may admit Nz=1, where z is in the direction of thickness, following that Nx=Ny=0. The overall demagnetizing field is, then, almost null, for any direction in the plane of the sheet (plane xy). This has important implication: we may suppose that the Magnetization of the grains inside the sheet is in the same plane of the sheet, as well as the Applied Field. We may also suppose that the directions of both vectors: applied field and magnetization are very near. This means that many predictions of this simple model (Eq. (18) to (27) apply for sheets.

However, we also have to remember that for polycrystalline materials there is interaction between neighbor grains, and this, no doubt, is source of error when comparing results from the model to real materials.

In particular, magnetic flux tends to pass through easy axis of grains, and this implies that i) flux may "deviate" inside the material ii) the H for each grain can be different of applied H, i.e., grains with easy axis in favorable position may have H > applied H (and vice-versa). This was discussed by Lawton and Stewart [21].

In fact, there is an "error compensation" in steel sheets. As mentioned above, Nz ≈1 for sheets, following that Magnetization (B) and Applied Field (H) are in the same plane, the plane of the sheet. If we add all the B (where $B=\mu_0 H+ J$) vectors of all grains we get an average value. The direction of the vector "sum of all B of all grains" is near that of the applied field H.

Some other complications also increase the difficulty of this problem: each grain has different geometry and, besides, as already mentioned, each grain interacts with the neighbors. If all these complications have to be considered, only approximate solutions are possible. But, it appears that, as a 1st approximation, the effect of demagnetizing field can be neglected in sheets.

Another simplification is neglecting the existence of domains and domain walls [22], but for high fields (B_{25} and B_{50}), this assumption can be used.

Summarizing, Magnetic Induction can be scaled to magnetocrystalline anisotropy in high fields (B_{50} and B_{25}), but this is an approximation where effects of demagnetizing field and existence of domain walls were neglected.

3.2. Angular dependence of permeability

Permeability depends, approximately, on the inverse way to coercivity ($\mu \propto 1/Hc$), and this relation is especially valid for the case of initial permeability ($H \rightarrow 0$). For very small applied field, which is the case of initial permeability, domain wall displacement is more relevant [23]. For higher fields, domain rotation tends to dominate.

As permeability is result of both competing mechanisms (domain rotation and domain wall movement), it is very difficult to be modeled. However, coercivity Hc can be modeled, and the results used to interpret the angular dependence of the permeability. The angular dependence of coercivity is also very useful to understand the angular dependence of iron losses, subject of the next section.

Coercivity itself is quite complex: it is described as a sum of several factors [24]. Concerning the effect of inclusions, no anisotropy is predicted since the source of increase of coercivity is the magnetostatic energy associated with inclusions [25], which is an isotropic effect.

However, the effect of grain size may lead to severe anisotropy. The 1/Gs factor represents a kind of "frequency": each time that a new grain boundary, the reversal process has to happen again. Thus, the equation that relates coercive field and grain size Gs is:

$$\Delta Hc = (\mu_0 Ms)^{-1} (c\, K_1 + d\, \gamma_p)\ (1/Gs) \qquad (28)$$

where γ_p *is* the domain wall energy. The dimensionless *c* and *d* are to be experimentally determined. Decreasing grain size, the ratio *c/d* increases, because domain rotation becomes more important for small grain size. The *c* and *d* variables also have angular dependence, as it will be discussed below. The concept of "stable nucleus", as introduced by Doring [26] could be used to estimate the magnitude of *d*.

The angular dependence of d (the case of resistance against domain wall displacement) is given by the Kondorsky law (Eq. 29), where φ is the angle between H, the applied field, and the direction of the magnetization vector of the domain:

$$H_c(\varphi) = \frac{1}{\cos\varphi} \tag{29}$$

The angular dependence of c is quite complicated. Nevertheless, the deduction below shows it is related to magnetocrystalline anisotropy. This discussion also illustrates the complexity of this question.

The formulation of a Stoner-Wohlfarth model for cubic crystals is not simple. Solutions are found for particular situations. The example that will be shown is for a {100} plane, which is simple to be studied. In this particular case, two of the crystal easy axis, applied field and Magnetization lie on the same plane (see Fig. 3). This case is called "biaxial anisotropy" [27].

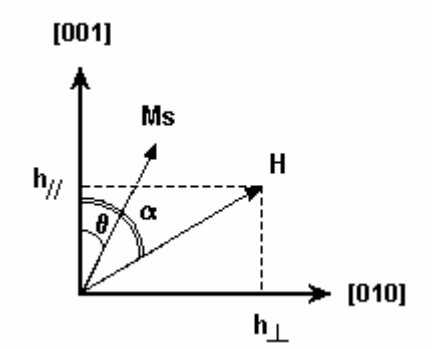

Fig. 3.. Relationship between angles α and θ, applied field H, magnetization and saturation Ms and easy axis in a cubic crystal. Biaxial anisotropy is the particular case where 2 easy axis, Ms, H lie on the same plane (100)

Equations (30) to (35) are the result of the Stoner-Wohlfarth model for the particular case of Fig. 3 (α is the angle between H and easy axis and θ is the angle between Ms and the easy axis). It can be seen that (α - θ = φ).

$$E = \frac{K_1}{4}\text{sen}^2(2\theta) - \mu_0 M_s H\cos(\alpha-\theta) \tag{30}$$

$$\frac{dE}{d\theta} = \frac{K_1}{2}\text{sen}(4\theta) - \mu_0 M_s H\,\text{sen}(\alpha-\theta) \tag{31}$$

$$\frac{d^2E}{d\theta^2} = 2K_1\cos(4\theta) + \mu_0 M_s H\cos(\alpha-\theta) \tag{32}$$

After simplifying Eq. 30 with the relations: $\mu_0 M_s H = h$; $h_{//} = h\,sen\,\alpha$; $h_{\perp} = h\cos\alpha$:

$$E = \frac{K_1}{4}\text{sen}^2(2\theta) - h_{\perp}\,\text{sen}\,\theta - h_{//}\cos\theta \tag{33}$$

the critical field for magnetization reversal is found for $dE/d\theta = 0$, $d^2E/d\theta^2 = 0$:

$$h_{\perp} = 5\,sen^3\,\theta - 6\cos^5\theta \tag{34a}$$

$$h_{//} = 5\cos^3\theta - 6\,sen^5\,\theta \tag{34b}$$

Equations (34a and 34b) allow to obtain, parametrically, $h(\theta)$ see Fig. 4.

The magnetization M is zero when M=Ms cos (α - θ) =0, i.e., (α - θ) =π/2. The magnetization is, thus, 0 for

$$H_c = \frac{2K_1}{\mu_0 M_s}\frac{sen4\theta}{4} \tag{35}$$

The equation (35) gives the dependence Hc (θ) in higher angles, i.e., $\frac{\pi}{8} \le \theta \le \frac{\pi}{4}$. Thus, for a plane (100), in the case of coherent rotation (Stoner-Wohlfarth model), equations (34a and 34b) apply for the range $0 \le \theta \le \pi/8$, while equation (35) applies for the range $\pi/8 \le \theta \le \pi/4$.

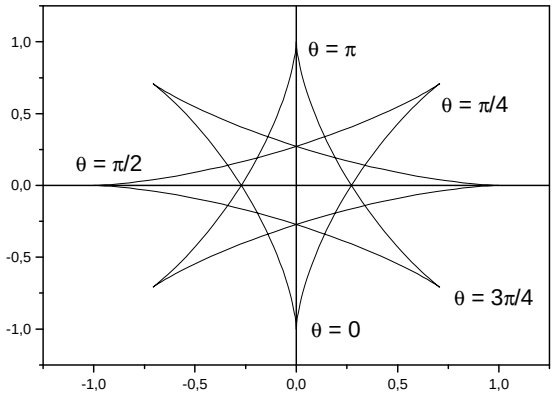

Fig. 4. Critical field for reversal of magnetization as function of angle θ (case of irreversible rotation) "Wind Rose", calculated according equations 34a and 34b.

Summarizing, there is a "competition" between domain wall displacement and rotation. Both mechanisms together determine the Hc. For lower φ angles, the moving of domain walls is more relevant (the 1/cos φ law). For higher angles, with applied field H far from the easy axis, rotation becomes more important.

As consequence of the existence of both contributions - rotation and domain wall movement - coercivity and also permeability are not direct functions of the magnetocrystalline anisotropy.

3.3. Angular dependence of the iron losses

According the Loss Separation Model [17, 28], the total losses are $P_t = P_h + P_{cl} + P_{an}$, where P_h is hysteresis losses, P_{cl} is classical, P_{an} is anomalous. P_h is the area of the hysteresis curve times the frequency f:

$$P_h = f\oint BdH \tag{36}$$

The area of hysteresis curve can be approximated as area= 4 B_{max} Hc, especially if the hysteresis curve has rectangular shape. This implies that, for a rectangular loop, Ph is directly proportional to Hc.

$$P_h = 4\,fB_{\max}H_c \tag{37}$$

The eddy losses P_{cl} are given by the "classical"

expression [29], Eq. (38), for sinusoidal waveform:

$$P_{cl} = \frac{\pi^2 f^2 B_{\max}^2 e^2}{6\rho} \quad (38)$$

where e is thickness and ρ is resistivity. The anomalous component, $P_{an,}$ is found by the difference $P_{an}=P_t-P_h-P_{cl}$., and can be estimated with the E.q (3) [30,31]:

$$P_{an} = a_3 \cdot Gs^{1/2} \cdot \frac{1}{\rho} \cdot e^2 \cdot B_{\max}^2 \cdot f^{3/2} \quad (39)$$

Pry and Bean model [32] predicts that $P_{an} \propto D/e$, where D is the distance between domain walls. As $n \propto 1/D$, Eq. 3 can be modified to:

$$P_{an} = a_4 \cdot \frac{1}{n} \cdot Gs^{1/2} \cdot \frac{1}{\rho} \cdot e^2 \cdot B_{\max}^2 \cdot f^{3/2} \quad (40)$$

where $a_3 = a_4/n$ (n is non-dimensional)

In fact, n varies according the plane and direction. Thus, the distance between domain walls (n) changes with crystalline orientation and this generates an anisotropy that is not related to magnetocrystalline anisotropy.

It has been proposed [33,34] that even iron losses could be scaled to Eq. (1). But, as can be seen from Eq. (37) and Eq. (40), this suggestion [33,34] is not a very good approximation, because Eq. (37) and (40), which can describe anisotropy of iron losses, are not directly related to magnetocrystalline anisotropy. Processes of domain wall displacement, represented by the Kondorsky law (Eq. 29) Hc = 1/cos φ, are the main reason for the non-agreement. As an additional source of anisotropy, Birsan and Szpunar [33] suggested also "grain shape anisotropy", besides texture, and this can be inferred, and estimated, from Eq. (28), (37) and (40).

CONCLUSIONS

Theoretical analysis is a valuable allied of Metrology, since it can help to identify sources of error and indicates the path to be followed by the experimental approach.

A mathematical deduction from the ODF – Orientation Distribution Function - Theory indicates that the experimental measurement of magnetic properties at 0^o, 45^o, 90^o for the Rolling Direction (RD) can be used to estimate the average magnetic properties of the entire steel sheet. This theoretical result is consequence of the symmetries of steel sheets, i.e., the crystalline symmetry of bcc iron and orthorhombic symmetry of sheet.

Magnetic Induction (B_{50} and B_{25}) can be scaled to magnetocrystalline anisotropy and, thus, can be described by an equation of the type $A = A_o + A_1 \cos(2\beta) + A_2 \cos(4\beta)$, where β is the angle towards Rolling Direction (RD).

Permeability and iron losses depend, in part, on magnetocrystalline anisotropy and, in another part, on domain wall displacement processes. Moreover, iron losses depend on the entire domain structure in the sample. After a critical analysis, it appears possible that permeability and iron losses can be described, as an approximation, by an equation of type $A = A_o + A_1 \cos(2\beta) + A_2 \cos(4\beta)$, hypothesis to be experimentally tested.

ACKNOWLEDGEMENTS

CNPq – PROMETRO, CNPq – CTENERG and FINEP.

REFERENCES

[1] J. P. Santos, F. J.G. Landgraf, G. C. Guimarães, J. Magn. Magn. Mat., in press.
[2] A. Honda, B. Fukuda, I. Ohyama, Y. Mine. J. Mat. Eng. Vol. 12, No. 1, pp. 41-45, 1990.
[3] M. F. de Campos, F. J. G. Landgraf, I. G. S. Falleiros, G. C. Fronzaglia, H. Kahn. ISIJ Int. Vol. 44, No. 10, pp. 1733-1737, 2004
[4] M. F. de Campos, F. J. G. Landgraf, R. Takanohashi, F. C. Chagas, I. G. S. Falleiros, G. C. Fronzaglia, H. Kahn. ISIJ Int. Vol. 44, No. 3, pp. 591-597, 2004
[5] M. F. de Campos, A. P. Tschiptschin, F. J. G. Landgraf. J. Magn. Magn. Mat. Vol. 226, pp. 1536-1538, 2001.
[6] ASTM Standard A343 / A343 M 03. Originally approved in 1949.Current edition approved June 10, 2003. Published July 2003.
[7] Norma ABNT - NBR 5161 (JULHO 1977) revalidada em MAIO 1996.
[8] H.-J. Bunge "Texture analysis in materials science – mathematical methods". London, Butterworths, 1982.
[9] H.-J. Bunge. Steel. Res. Vol. 62, pp. 530-541, 1991.
[10] M. I. Darby, E. D. Isaac. IEEE Trans. Magn. Vol. MAG-10, pp. 259-304, 1974.
[11] M. Birsan, J. A. Szpunar. Mat. Sci. Forum. Vol. 157-162, pp. 1543-1550, 1994.
[12] K.-H. Jackel, J. Tobisch, K. Kleinstuck. Elektrie, Vol. 39, pp. 405-406, 1985.
[13] H.-J. Bunge In: "Advances and applications of quantitative texture analysis", H. J. Bunge, C. Esling, editors.. Clausthal, FRG, 1989. Oberursel, FRG, DGM Informationsgesellschaft – Verlag, 1991. p. 3-18.
[14] M. Yashiki, H. Okamoto, IEEE Trans. Magn. **23** (1987) 3086.
[15] T. Yonamine, M. F. de Campos, N. A. Castro, F. J. G. Landgraf, "Modelling magnetic polarisation J_{50} by different methods" J. Magn Magn Mater, in press.
[16] L. Neél. J. Phys. Radium, Vol. 5, pp. 241, 1944.
[17] F. Brailsford. Physical principles of magnetism. London, Van Nostrand, 1966.
[18] K. H. Stewart. Ferromagnetic domains, UK, University of Cambridge, 1954.
[19] R. M. Del Vecchio. J. Appl. Phys., Vol. 55, pp. 2186-2188, 1984.
[20] H. Lawton, K. H Stewart. Proc. Roy. Soc. A, V. 193 , P. 72-88, 1948.
[21] H. Lawton, K. H Stewart. Proc. Phys. Soc. A, V. 63 , p. 848-851, 1950.
[22] J. D. Sievert, C. Voigt. Phys. Stat. Sol. (A) Vol. 37, pp. 205-209, 1976.
[23] S. Chikazumi, Physics of magnetism. New York, John Wiley & Sons, 1964.
[24] E. Adler, H. Pfeiffer. IEEE Trans. Magn. Vol. MAG-10, pp. 172-174, 1974.
[25] M. F. de Campos, M. Emura, F. J. G. Landgraf, "Consequences of magnetic aging for iron losses in electrical steels" J. Magn Magn Mater, in press.
[26] W. Doring. Zeitschrift fur Phys. Vol. 108, pp. 137-152, 1938.
[27] G. Bertotti, Hysteresis in Magnetism. Academic Press, San Diego, 1998.
[28] R. Boll, Weichmagnetische Werkstoffe. Vacuumschmelze, Hanau, Germany, 1990 (in German).
[29] K. L. Scott. Proc. of Inst.Electrical Engineers, Vol. 18, pp. 1750-1764, 1930.
[30] M. F. de Campos, J. C. Teixeira, F. J. G. Landgraf , J. Magn Magn Mater, 301, pp. 94-99, 2006.
[31] M. F. de Campos, T. Yonamine, M. Fukuhara, F.J.G Landgraf, C. A. Achete, F. P. Missell. "Effect of frequency on the iron losses of 0.5% and 1.5%Si non-oriented electrical steels", IEEE Trans. Magn., accepted for publication.
[32] R. H. Pry, C.P. Bean, J. Appl. Phys., vol. 29, pp. 532-533 1958.
[33] M. Birsan, J. A. Szpunar. J. Appl. Phys., Vol. 81, pp. 821-823, 1997.
[34] M. Birsan, J. A. Szpunar. J. Appl. Phys., Vol. 80, pp. 6915-6919, 1996.